Supporting Information for

Molecular Mechanism of Polycation-Induced Pore Formation in Biomembranes

Neha Awasthi,[,†] Wojciech Kopec,[‡,⊥] Natalia Wilkosz,[‡] Dorota Jamróz,[‡] Jochen S. Hub,[†] Maria Zatorska,[‡] Rafał Petka,[‡] Maria Nowakowska,[‡] and Mariusz Kepczynski*[,‡]*

[†]Institute for Microbiology and Genetics, Georg-August-Universität, Justus-von-Liebig Weg 11, 37077 Göttingen, Germany

[‡]Jagiellonian University, Faculty of Chemistry, Gronostajowa 2, 30-387 Kraków, Poland

Number of pages: 15

Number of figures: 10

Number of tables: 3

1. MD simulations

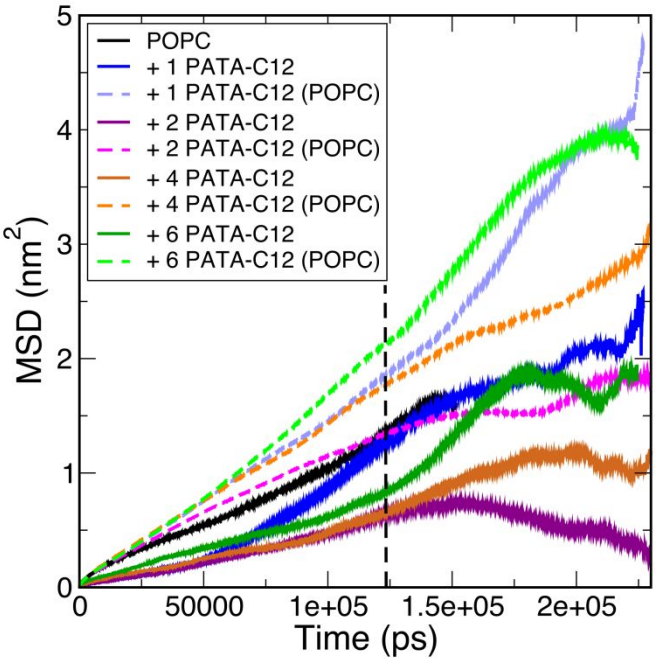

Figure S1. Mean Square Displacement (MSD) for POPC (dashed lines) and PATA-C12 molecules (solid lines) for systems **M1-M8** (see Table 1 for system details). The black vertical dashed line at ~125 ns indicates the time limit up to which linear regression was performed to calculate Diffusion constant (D) for POPC and PATA-C12 molecules. Respective D values are shown in Table 2 in the main text.

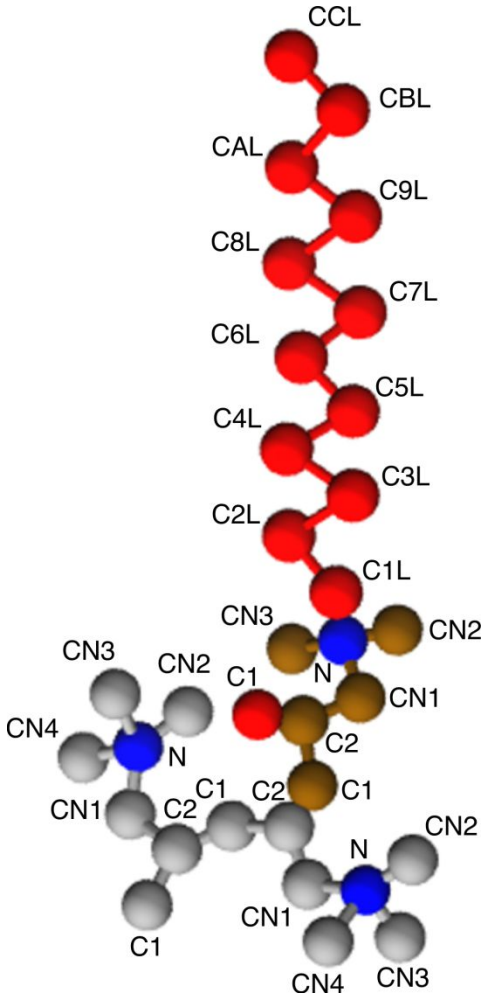

Figure S2. A single allyltrimethylammonium unit of the PATA C-12 molecule. along with the atom names used. Atom types and associated charges are provided in Table S1.

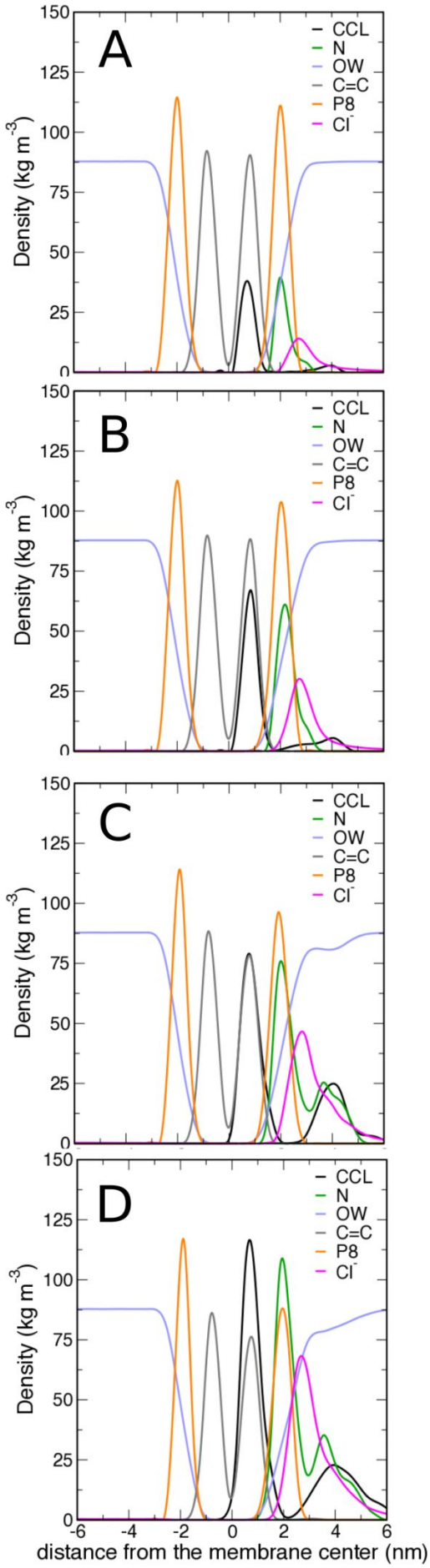

Figure S3. Scaled mass density profiles of PATA-C12 (the N atoms and the terminal CH_3 groups of dodecyl chains). the selected POPC groups (double bonds and phosphate groups). chloride anions, and water along the bilayer normal averaged over the whole trajectories for systems **M1** (A). **M2** (B). **M4** (C). and **M6** (D). Densities for OW were scaled by 0.1 and those of CCL and N by 10.

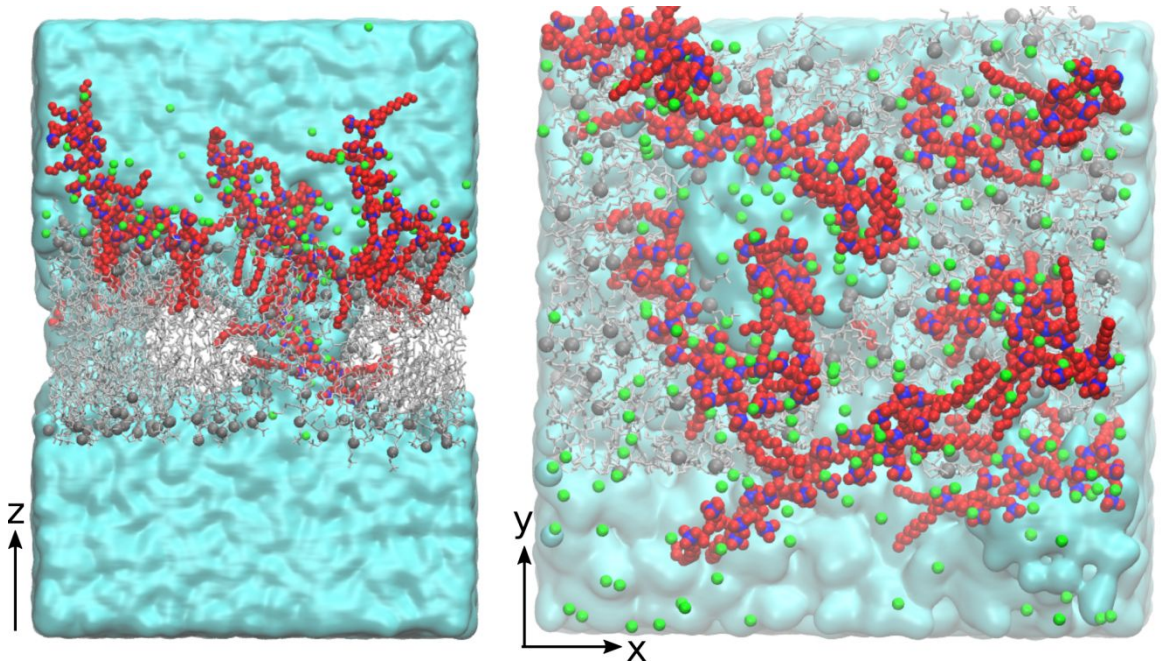

Figure S4. Simulation snapshots showing the spontaneous formation of pores in the POPC membrane in the presence of N = 8 PATA-C12 molecules (system **M8**). Two large water-filled pores are formed within 50 ns of simulation. Lipids are shown as silver sticks. and their phosphate groups are shown as grey spheres. PATA-C12 molecules are shown in red. nitrogen atoms of the polymer in blue. Chloride ions are presented as green spheres and water in cyan.

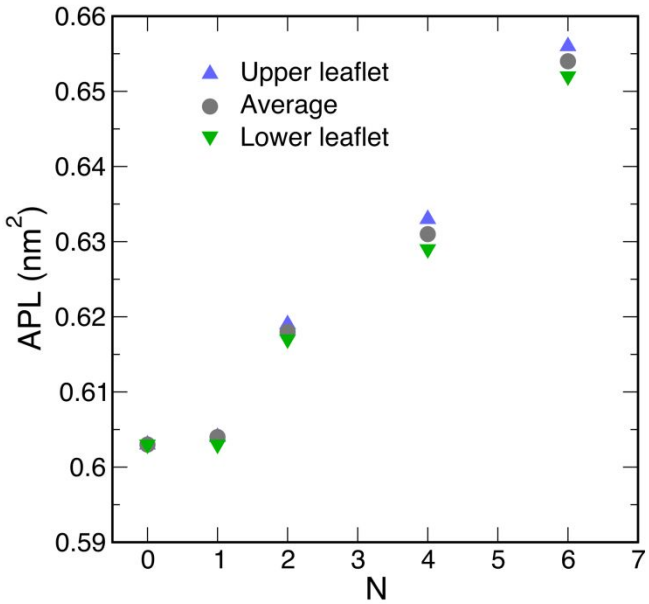

Figure S5. Area per lipid (APL) for the inner and outer POPC membrane leaflets calculated for different PATA-C12 content. N where N denotes the number of PATA-C12 molecules present in the simulation system. The polycation molecules are embedded in the outer (upper) leaflet.

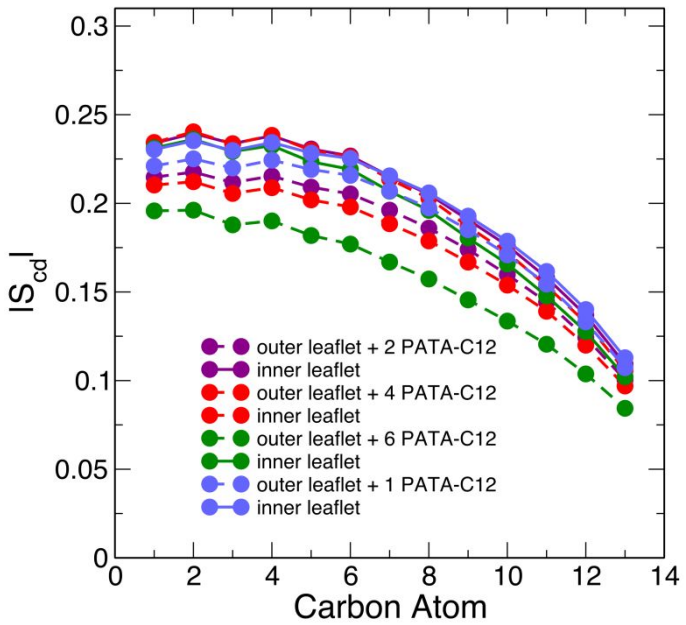

Figure S6. Leaflet specific deuterium order parameter. $|S_{CD}|$. for the POPC palmitoyl chains. Data is shown for one out of the three equilibrium trajectories for each *N*. Order parameters for the remaining two trajectories show the same trend.

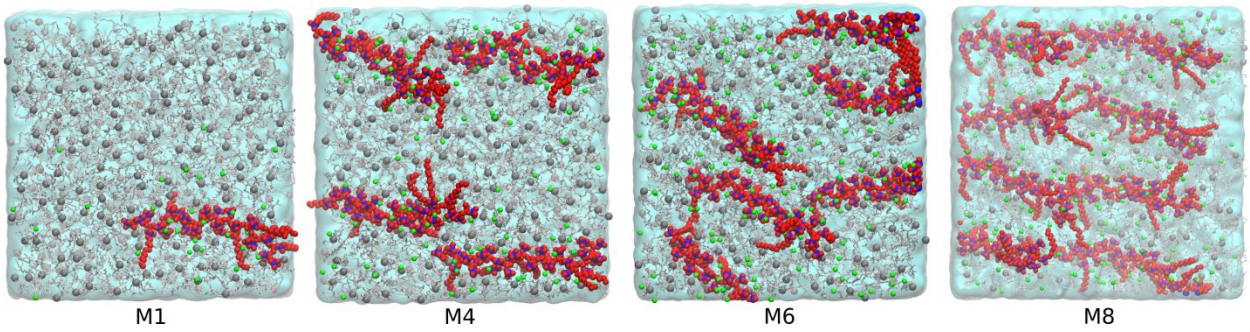

Figure S7. Simulation snapshots (top view) from long equilibrium simulations showing PATA-C12 coverage on the membrane. These snapshots refer to the starting structures for umbrella sampling simulations (**UmbrellaM1-UmbrallaM8**). The PATA-C12 molecule is shown as red spheres with the nitrogen atoms in blue. Lipids are shown as grey sticks. and their phosphate groups are shown as grey spheres. Chloride ions are represented by green spheres.

Table S1. Atom names. types and charges used for simulations of PATA C-12.

Atom name	Atom type	Atom charge
C1	LC2	0.0
C2	LC1	0.0
CN1	LH2	0.3
N	LNL	-0.5
CN2	LC3	0.4
CN3	LC3	0.4
CN4	LC3	0.4
C1L	LH2	0.35
C2L	LP2	0.35
C3L	LP2	0.0
C4L	LP2	0.0
C5L	LP2	0.0
C6L	LP2	0.0
C7L	LP2	0.0
C8L	LP2	0.0
C9L	LP2	0.0
CAL	LP2	0.0
CBL	LP2	0.0
CCL	LP3	0.0

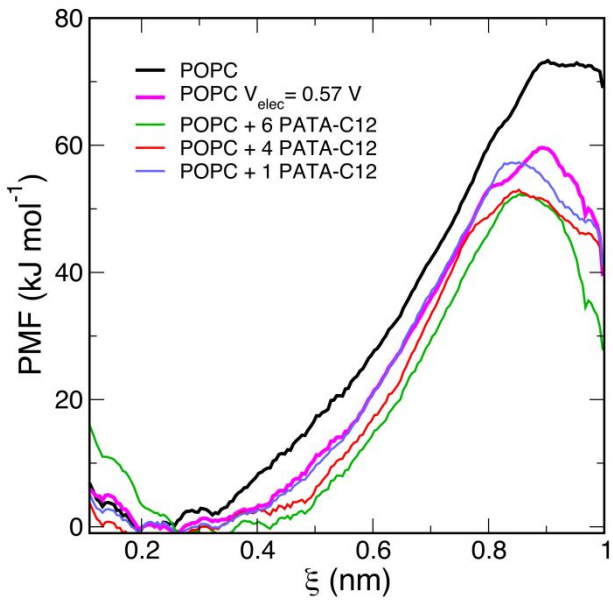

Figure S8. PMFs for pore nucleation in POPC membranes using the slice coordinate: the role of applied electric field. Umbrella sampling simulations were performed for a transmembrane voltage (V_{elec}) of ~0.57 V, and the corresponding PMF is shown in magenta. For reference, PMFs for the pure POPC membrane (black curve) and for POPC membranes with different number of PATA-C12 molecules adsorbed on the outer leaflet (blue/red/green curves) are also shown. All PMFs show nucleation barriers for pore formation. Applying the transmembrane voltage or the addition of PATA-C12 molecules, both, a) reduce the nucleation barrier for pore formation, and b) lower the free energy for pore formation (ΔG_{pore}) as compared to the pure POPC membrane (black curve). All PMFs were computed from the 30 ns trajectory for each umbrella window for the respective umbrella sampling simulations. See Section 2 of the Supporting Information for further details.

2. Free energy of pore formation in the presence of an applied electric field

Does the asymmetric adhesion positively charged polycation molecules induce pore formation in a mechanism *similar* to pore formation in the presence of an applied electric field across the membrane? In order to address this question, we performed an additional umbrella sampling simulation for the pure POPC with an applied electric field of 0.04 V/nm using the slice coordinate. This field corresponds to a transmembrane electrostatic potential difference of ~0.57 V (simulation box ~14.34 nm along the z-direction). Each umbrella window was simulated for

30 ns. To be consistent, all PMFs shown in Figure S8 were computed from the 30 ns trajectory for each umbrella window of the respective umbrella sampling simulations. All other simulation parameters were identical to those used for the PMF calculations in Figure 8 (main text), and described in methods (main text).

Figure S8 shows the PMFs for the pure POPC membrane (black curve), the pure POPC membrane with a transmembrane voltage (V_{elec}) of ~0.57V (magenta curve), and for POPC membranes with different PATA-C12 molecules adsorbed on the outer leaflet (blue/red/green curves). We observe that all PMFs for different concentration of polycation molecules (Figure S8, blue, red and green curves) are rather *similar* to the PMF calculated in the presence of a transmembrane voltage (Figure S8, magenta curve).

We find that applying a transmembrane voltage lowers the free energy for pore formation (ΔG_{pore}), in agreement with previous MD simulations on electroporation,[1,2,3,4] and also lowers the nucleation barrier for pore formation. In the presence of a transmembrane voltage, pore formation is favored due to asymmetrical changes in the preferred dipole orientations of lipids and water molecules. Presence of such an external voltage across the membrane results in asymmetrical electric fields, especially in the transition region between the hydrophobic core and the hydrophilic headgroup region.[2] It has been suggested that such field gradients at the interface lipid headgroup/hydrophobic core effectively decrease the nucleation barrier for pore formation.[2] We find that ΔG_{pore} for a pure POPC membrane in the presence of V_{elec} is ~40 kJ mol^{-1} (Figure S8/magenta curve), and is very similar to ΔG_{pore} obtained in the presence of 1 or 4 PATA-C12 molecules (Figure S8/blue and red curves, respectively). The nucleation barrier for pore formation in a pure POPC membrane in the presence of V_{elec} (~60 kJ mol^{-1}, Figure S8/magenta

curve) is close to that for a POPC membrane with 1 adsorbed PATA-C12 molecule (~58 kJ mol^{-1}, Figure S8/blue curve).

Taken together, these PMFs support our hypothesis that the asymmetric adhesion of positively charged PATA-C12 molecules drives pore formation via a mechanism similar to electroporation. More quantitative comparison and further analysis will be presented in a future work.

3. Determination of the critical micellar concentration (CMC) for PATA-C12.

The CMC value for the polycation was determined using a fluorescent molecular probe technique as described previously.[5] A stock solution of 1,6-diphenyl-1,3,5-hexatriene (DPH, Aldrich) was prepared in methanol at a concentration of 0.4 mM by short sonication in a bath sonicator. A series of samples containing PATA-C12 at various concentrations (in a range of 0 – 0.1 mg/mL) and a constant DPH concentration (4 μM) were prepared and stirred for 4 hours in the dark. The fluorescence spectra of these samples were measured using a LS-55 Fluorescence Spectrometer (Perkin-Elmer). The samples were excited at 350 nm. Figure S9 shows the dependence of the fluorescence intensity at 440 nm on the PATA-C12 concentration (in logarithmic scale). The CMC value was determined to be 0.029 ± 0.002 mg/mL from the intersection of two lines fitted to two regions defined for low polymer concentration and when the DPH fluorescence intensity increased abruptly (see Figure S9).

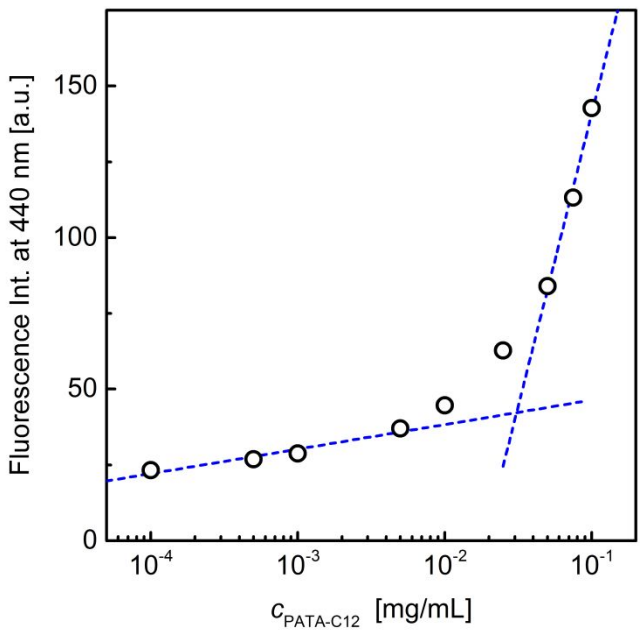

Figure S9. The fluorescence intensity of DPH (c_{DPH} = 4 μM, λ_{ex} = 350 nm) at 440 nm as a function of the PATA-C12 concentration.

4. Dynamic light scattering (DLS) and nanoparticle tracking analysis (NTA) measurements

A series of samples containing liposomes (c_{POPC} = 0.5 mg/mL) and PATA-C12 in a concentration range of 0 – 0.08 mg/mL were prepared. A Malvern Nano ZS light-scattering apparatus (Malvern Instrument Ltd., Worcestershire, UK) was used for dynamic light scattering (DLS) measurements. The measurements were performed as previously described.[6] The attenuator and the measurement position in the cell were set to 7 and 4.65 mm, respectively, for all samples to enable the count rates to be compared. The results (Table S2) show that the liposome sizes and the count rates increased slightly as the PATA-C12 concentration in the system increased. Since the size of the objects in the samples changed only slightly, it is reasonable to assume that the count rate values are proportional to the number of objects present in the dispersion. Thus, it can be concluded that the number of lipid vesicles did not decrease upon treatment with PATA-C12 in the range of polymer concentrations studied.

An NS500 NanoSight instrument (Malvern) was used for nanoparticle tracking analysis (NTA). The measurements were performed at 25°C as described previously.[7] The samples were diluted 500 times for the measurements. The results are collected in Table S3. The sizes of liposomes are in good agreement with the values obtained in the DLS experiments. The particle concentration changed with the increase in polycation concentration, but for $c_{\text{PATA-C12}} \leq 0.01$ mg/L, the number of the objects is not lower than that for the pristine liposomes.

Table S2. The values of the mean hydrodynamic diameter (d*z*), dispersity (DI) and the Mean Count Rate of POPC liposomes (c_{POPC} = 0.5 mg/mL) dispersed in a 1 mM NaCl solution treated with PATA-C12 (values are the mean ± standard deviation) obtained from the DLS measurements.

PATA-C12 concentration [μg/mL]	PATA-C12 content[a] [wt%]	d*z* [nm] (*n* = 5)	DI (*n* = 5)	Mean Count Rate [kcps][b] (*n* = 5)
0	0	123.7 ± 2.0	0.087 ± 0.042	333.8 ± 2.8
10	2	124.0 ± 1.9	0.11 ± 0.021	337.3 ± 2.8
20	4	124.2 ± 1.6	0.094 ± 0.029	338.9 ± 3.9
30	6	124.8 ± 1.9	0.132 ± 0.02	361.1 ± 3.4
40	8	124.4 ± 2.0	0.113 ± 0.042	352.3 ± 2.2
80	16	127.8 ± 1.4	0.13 ± 0.02	362.7 ± 5.9

[a] Weight polycation fractions with respect to the lipid content.
[b] The mean count rate during the measurement is 1000 photons (counts) per sec = 1 kcps.

Table S3. The values of the modal particle size (d*m*) and the concentration of nanoparticles in suspension of POPC liposomes (c_{POPC} = 0.5 mg/mL) dispersed in a 1 mM NaCl solution and treated with PATA-C12 (values are the mean ± standard deviation) obtained from the NTA measurements.

PATA-C12 concentration [μg/mL]	PATA-C12 content[a] [wt%]	d*m* [nm] (n = 5)	Particle concentration [particles/mL] (n = 5)
0	0	111.4 ± 1.7	(1.58 ± 0.04) × 10^9
10	2	120.5 ± 1.7	(1.86 ± 0.04) × 10^9
80	16	126.3 ± 3.1	(1.31 ± 0.13) × 10^9

[a] Weight polycation fractions with respect to the lipid content.

5. Atomic Force Microscopy (AFM) Measurements

AFM observation of supported POPC bilayers were performed before and after addition of PATA-C12 (Figure S10). The AFM images show that the polycation induces the formation of new nanoscale holes in the bilayer. Additionally, some areas of the bilayer have a reduced thickness after treatment with the polycation. This indicates that PATA-C12 is probably adsorbed unevenly on the membrane surface, creating patches with reduced thickness.

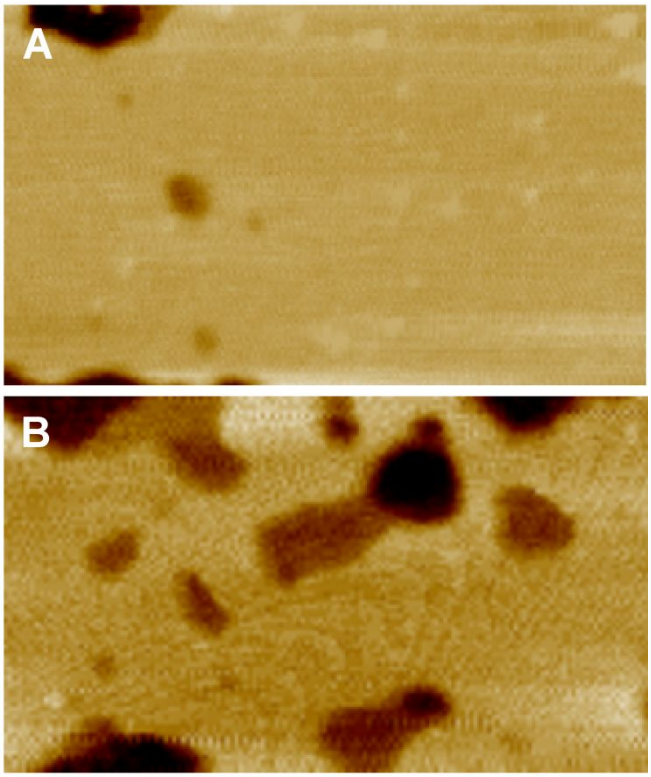

Figure S10. Height images from Picoforce mode AFM measurements in water of the POPC bilayer immobilized on the silicon surface before (A) and after (B) addition of PATA-C12 (0.005 mg/mL). Black areas are holes in the membrane and dark brown areas are regions of the membrane with reduced thickness. The image sizes are 0.85 µm - 0.5 µm.

REFERENCES

(1) Tieleman, D. P.; Leontiadou, H.; Mark, A. E.; Marrink, S.-J. Simulation of Pore Formation in Lipid Bilayers by Mechanical Stress and Electric Fields. *J. Am. Chem. Soc.*, **2003**, *125* (21), 6382–6383. DOI: 10.1021/ja029504i

(2) Tieleman, D. P. The molecular basis of electroporation. *BMC Biochemistry*, **2004**, *5*, 10. DOI: 10.1186/1471-2091-5-10

(3) Tarek, M. Membrane electroporation: a molecular dynamics simulation. *Biophys. J.* **2005***, 88* (6), 4045–4053. DOI: 10.1529/biophysj.104.050617

(4) Ziegler, M. J.; Vernier, P. T. Interface water dynamics and porating electric fields for phospholipid bilayers. *J. Phys. Chem. B*, **2008**, *112* (43), 13588–13596. DOI: 10.1021/jp8027726

(5) Chattopadhyay, A.; London, E. Fluorimetric determination of critical micelle concentration avoiding interference from detergent charge. *Anal. Biochem*. **1984**, *139* (2), 408–412. DOI: 10.1016/0003-2697(84)90026-5

(6) Kepczynski, M.; Nawalany, K.; Jachimska, B.; Romek, M.; Nowakowska, M. Pegylated Tetraarylporphyrin Entrapped in Liposomal Membranes. A possible Novel Drug-Carrier System for Photodynamic Therapy. *Colloids Surf., B* **2006**, *49*, 22–30. DOI: 10.1016/j.colsurfb.2006.02.008

(7) Szczepanowicz, K.; Bzowska, M.; Kruk, T.; Karabasz, A.; Bereta, J.; Warszynski, P. Pegylated polyelectrolyte nanoparticles containing paclitaxel as apromising candidate for drug carriers for passive targeting. *Colloids Surf. B* **2016**, *143*, 463–471. DOI: 10.1016/j.colsurfb.2016.03.064